Cannabidiol is a negative allosteric modulator of the type 1 cannabinoid receptor.

R B Laprairie[1], A M Bagher[1], M E M Kelly[1,2], E M Denovan-Wright[1]*

[1]Departments of Pharmacology and [2]Opthamology and Visual Sciences, Dalhousie University, Halifax NS Canada B3H 4R2

Running title: Negative allosteric modulation of CB1 by cannabidiol

Address for Correspondence:
Eileen M Denovan-Wright, PhD
Department of Pharmacology,
Dalhousie University,
Rm 6E 5850 College St.
Halifax NS Canada B3H 4R2
E-mail: emdenova@dal.ca
Phone: 1.902.494.1363
Fax: 1.902.494.1388

This article has been accepted for publication and undergone full peer review but has not been through the copyediting, typesetting, pagination and proofreading process which may lead to differences between this version and the Version of Record. Please cite this article as doi: 10.1002/bph.13250

Author Contribution Statement

- RB Laprairie performed the research.
- RB Laprairie, AM Bagher and EM Denovan-Wright designed the research study.
- MEM Kelly and AM Bagher contributed essential reagents and tools.
- RB Laprairie analysed the data.
- RB Laprairie, MEM Kelly and EM Denovan-Wright wrote the paper.

Word Count: 5,497

Abbreviations:

2-AG, 2-arachidonyl glycerol;
6aR,10aR)-3-(1-methanesulfonylamino-4-hexyn-6-yl)-6a,7,10,10a-tetrahydro-6,6,9-trimethyl-6H-dibenzo[b,d]pyran, O-2050;
ANOVA, analysis of variance;
BRET, bioluminescence resonance energy transfer;
$BRET_{Eff}$, BRET efficiency
CB_1, type 1 cannabinoid receptor;
CB_2, type 2 cannabinoid receptor;
CBD, cannabidiol;
CRC, concentration-response curve
FAAH, fatty acid amide hydrolase;
GPCR, G protein-coupled receptor
HEK 293A cells, human embryonic kidney 293A cells;
HERG, human ether-a-go-go-related-gene;
NAM, negative allosteric modulator;
PAM, positive allosteric modulator;
PPARγ, peroxisome proliferator-activated receptor γ;
SEM, standard error of the mean;
THC, Δ^9-tetrahydrocannabinol;
TRPV1, transient receptor potential cation channel subfamily V 1;

Abstract

Background and purpose

Cannabidiol has been reported to act as an antagonist of cannabinoid agonists at type 1 cannabinoid receptors (CB_1). We hypothesized that cannabidiol can inhibit cannabinoid agonist activity through negative allosteric modulation of CB_1.

Experimental approach

CB_1 internalization, arrestin2 recruitment, and PLCβ3 and ERK1/2 phosphorylation, were quantified in HEK 293A cells heterologously expressing CB_1 and in the ST*Hdh*$^{Q7/Q7}$ cell model of striatal neurons endogenously expressing CB_1. Cells were treated with 2-arachidonylglycerol or Δ^9-tetrahydrocannabinol alone and in combination with different concentrations of cannabidiol.

Key results

Cannabidiol reduced the efficacy and potency of 2-arachidonylglycerol and Δ^9-tetrahydrocannabinol on PLCβ3- and ERK1/2-dependent signaling in cells heterologously (HEK 293A) or endogenously (ST*Hdh*$^{Q7/Q7}$) expressing CB_1. By reducing arrestin2 recruitment to CB_1, cannabidiol treatment prevented CB_1 internalization. The allosteric activity of cannabidiol depended upon polar residues being present at positions 98 and 107 in the extracellular amino-terminus.

Conclusions and implications

Cannabidiol behaved as a non-competitive negative allosteric modulator of CB_1. Allosteric modulation, in conjunction with non-CB_1 effects, may explain the *in vivo* effects of cannabidiol. Allosteric modulators of CB_1 have the potential to treat central nervous system and peripheral disorders while avoiding the adverse effects associated with orthosteric agonism or antagonism of CB_1.

Keywords

2-arachidonylglycerol, Cannabinoid, Cannabidiol, CB1, Allosteric modulator, Tetrahydrocannabinol

Introduction

Allosteric modulation of CB_1

The majority of available drugs that target G protein-coupled receptors (GPCR) act at the receptor's orthosteric site – the site at which the endogenous ligand binds (Christopoulos and Kenakin, 2002). The type 1 cannabinoid receptor (CB_1) is the most abundant GPCR in the central nervous system and is expressed throughout the periphery (reviewed in Ross, 2007; Pertwee, 2008). Orthosteric ligands of CB_1 have been touted as possible treatments for anxiety and depression, epilepsy, neurodegenerative diseases such as Huntington disease and Parkinson disease, and chronic pain (Pertwee, 2008; Piscitelli *et al*., 2012), and have been tested in the treatment of addiction, obesity, and diabetes (Pertwee, 2008; Piscitelli *et al*., 2012). Despite their therapeutic potential, orthosteric agonists of CB_1 are limited by their potential psychomimetic effects while orthosteric antagonists of CB_1 are limited by their depressant effects (Ross, 2007).

An allosteric binding site is a distinct domain from the orthosteric site that can bind to small molecules or other proteins in order to modulate receptor activity (Wootten *et al*., 2013). All class A, B, and C GPCRs investigated to date possess allosteric binding sites (Wootten *et al*., 2013). Ligands that bind to receptor allosteric sites may be classified as *allosteric agonists* that can activate a receptor independent of other ligands, *allosteric modulators* that alter the potency and efficacy of the orthosteric ligand but cannot activate the receptor alone, and *mixed agonist/modulator ligands*. As therapeutics, allosteric modulators, unlike allosteric agonists and mixed agonist/modulator ligands, are attractive because they lack intrinsic efficacy. Therefore, the effect ceiling of an allosteric modulator is determined by the endogenous or exogenous orthosteric ligand (Wooten *et al*., 2013). In contrast, exogenous orthosteric ligands may produce adverse effects through supra-physiological overactivation or down-regulation of a receptor (Wootten *et al*., 2013). Unlike orthosteric ligands, allosteric modulators of CB_1 may not produce these undesirable side effects because their efficacy depends on the presence of orthosteric ligands, such as the two major endocananbinoids anandamide and 2-arachidonylglycerol (2-AG) (Ross, 2007; Wootten *et al*, 2013).

To date, the best-characterized allosteric modulators of CB_1 are the positive allosteric modulator (PAM) Lipoxin A_4 (Pamplona *et al*., 2012) and the negative allosteric modulators (NAM) ORG27569 and PSNCBAM-1 (Price *et al*., 2005; Horswill *et al*., 2007; Wang *et al*., 2011; Ahn *et al*., 2013). ORG27569 and PSNCBAM-1 reduce the efficacy and potency of CB_1 agonists WIN55,212-2 and CP55,940 to stimulate $GTP\gamma S^{35}$, enhance $G\alpha_{i/o}$-dependent signaling and arrestin recruitment, and inhibit CB_1 internalization and cAMP accumulation at submicromolar concentrations (Price *et al*., 2005; Horswill *et al*., 2007; Wang *et al*., 2011; Ahn *et al*., 2013; Cawston *et al*., 2013). The well-characterized NAM activities of ORG27569 and PSNCBAM-1 are the archetypes against which novel CB_1 NAMs are compared.

Cannabidiol as a possible negative allosteric modulator of CB_1

Cannabidiol (CBD) is known to modulate the activity of many cellular effectors, including CB_1, the type 2 cannabinoid receptor (CB_2) (Hayakawa *et al*., 2008), the serotonin $5HT_{1A}$ receptor (Russo *et al*., 2005), GPR55 (Ryberg *et al*., 2007), the μ- and δ-opioid receptors (Kathmann *et al*., 2006), the transient receptor potential cation channel subfamily V 1 (TRPV1) (Bisogno *et al*., 2001), the peroxisome proliferator-activated receptor γ (PPARγ) (Campos *et al*., 2012), and fatty acid amide hydrolase (FAAH) (Bisogno *et al*., 2001). With regard to cannabinoid receptor-specific effects, several *in vitro* and *in vivo* studies have reported that CBD acts as an antagonist of cannabinoid agonists at CB_1 at doses well below the reported affinity (K_i) for CBD to the orthosteric agonist site of CB_1 (Pertwee *et al.*, 2002; Ryan *et al*., 2007; Thomas *et al*., 2007; McPartland *et al*., 2014). We recently reported that the effects of CBD on intracellular signaling were largely CB_1-independent (Laprairie *et al*.,

2014a). However, CBD inhibited CB_1 internalization *in vitro* at submicromolar concentrations where no other CB_1-dependent effect on signaling was observed (Laprairie *et al*., 2014a). Given the similarity with ORG27569 and PSNCBAM-1 inhibition of CB_1 internalization, and existing *in vivo* data suggesting CBD can act as a potent antagonist of CB_1 agonists, we hypothesized that CBD has NAM activity at CB_1.

Objective of this study

The objective of this study was to determine whether CBD had NAM activity at CB_1 *in vitro*. The NAM activity of CBD was tested for arrestin, $G\alpha_q$ (PLCβ3), and $G\alpha_{i/o}$ (ERK1/2) pathways using 2-AG and Δ^9-tetrahydrocannabinol (THC) as the orthosteric probes and compared to the competitive antagonist O-2050 (Hudson *et al*., 2010; Laprairie *et al*., 2014). While some studies have suggested O-2050 may be a partial agonist of CB_1 (Wiley *et al*., 2011, 2012), several groups have noted the competitive antagonistic activity of O-2050 at CB_1 (Canals and Milligan, 2008; Higuchi *et al.,* 2010; Ferreira *et al.*, 2012; Anderson *et al*., 2013). Allosteric effects of CBD were studied using an operational model of allosterism (Keov *et al*., 2011). Using this operational model, we were able to estimate ligand co-operativity (α), changes in efficacy (β), and orthosteric and allosteric ligand affinity (K_A and K_B) (Keov *et al*., 2011) and support our hypothesis that CBD displayed NAM activity at CB_1. HEK 293A and ST*Hdh*$^{Q7/Q7}$ cells were used to test our hypothesis. HEK 293A cells represent a well-characterized heterologous expression system to study CB_1 signaling while ST*Hdh*$^{Q7/Q7}$ cells model the major output of the indirect motor pathway of the striatum where CB_1 levels are highest relative to other regions of the brain (Tetrell *et al*., 2000; Laprairie *et al*., 2013, 2014a), making this cell line ideally suited to studying endocannabinoid signaling in a more physiologically relevant context.

Methods

Drugs

Drug stocks were made up in ethanol (THC) or DMSO [2-AG, CBD, and (6aR,10aR)-3-(1-methanesulfonylamino-4-hexyn-6-yl)-6a,7,10,10a-tetrahydro-6,6,9-trimethyl-6H-dibenzo[b,d]pyran (O-2050), *N*-(Piperidin-1-yl)-5-(4-iodophenyl)-1-(2,4-dichlorophenyl)-4-methyl-1*H*-pyrazole-3-carboxamide (AM251)] and diluted to final solvent concentrations of 0.1%. 2-AG, CBD, and O-2050 were purchased from Tocris Bioscience (Bristol, UK). THC was purchased from Sigma-Aldrich (Oakville, ON).

Cell culture

HEK 293A cells were from the American Type Culture Collection (ATCC, Manaassas, VI). Cells were maintained at 37°C, 5% CO_2 in DMEM supplemented with 10% FBS and 10^4 U mL^{-1} Pen/Strep.

ST*Hdh*$^{Q7/Q7}$ cells are derived from the conditionally immortalized striatal progenitor cells of embryonic day 14 C57BlJ/6 mice (Coriell Institute, Camden, NJ) (Tetrell *et al*., 2000). Cells were maintained at 33°C, 5% CO_2 in DMEM supplemented with 10% FBS, 2 mM L-glutamine, 10^4 U mL^{-1} Pen/Strep, and 400 μg mL^{-1} geneticin. Cells were serum-deprived for 24 h prior to experiments to promote differentiation (Tetrell *et al*., 2000; Laprairie *et al*., 2013, 2014a,b).

Plasmids and transfection

Human CB_1, CB_{1A}, CB_{1B}, and arrestin2 (β-arrestin1) were cloned and expressed as either green fluorescent protein^2 (GFP^2) or *Renilla* luciferase (Rluc) fusion proteins. CB_1-GFP^2, and arrestin2-Rluc were generated using the pGFP^2-N3 and pRluc-N1 plasmids (PerkinElmer, Waltham, MA) as described previously (Hudson *et al*., 2010; Laprairie *et al*., 2014a). The GFP^2-Rluc fusion construct, and Rluc plasmids have been previously described (Laprairie *et al*., 2014a).

The human CB_1 receptor was mutagenized at two cysteine residues (Cys-98 and Cys-

107). Mutagenesis was conducted as described previously (Laprairie *et al*. 2013) with the cysteine residues being mutated to alanines (C98A, C107A) or serines (C98S, C107S) using the CB_1-GFP^2 fusion plasmid and the following forward and reverse primers: CB_1^{C98A}-GFP^2 forward 5'-AACATCCAGGCTGGGGAGAACT-3', reverse 5'-AGTTCTCCCCAGCCTGGATGTT-3'; and CB_1^{C107A}-GFP^2 forward 5'-GACATAGAGGCTTTCATGGTC-3', reverse 5'-GACCATGAAAGCCTCTATGTC-3'; CB_1^{C98S}-GFP^2 forward 5'-AACATCCAGTCTGGGGAGAACT-3', reverse 5'-AGTTCTCCCCAGACTGGATGTT-3'; and CB_1^{C107S}-GFP^2 forward 5'-GACATAGAGTCTTTCATGGTC-3', reverse 5'-GACCATGAAAGACTCTATGTC-3'. Mutagenesis was confirmed by sequencing (GeneWiz, Camden, NJ).

Cells were grown in 6 well plates and transfected with 200 ng of the Rluc fusion plasmid and 400 ng of the GFP^2 fusion plasmid according to previously described protocols (Laprairie *et al*., 2014a) using Lipofectamine 2000® according to the manufacturer's instructions (Invitrogen, Burlington, ON). Transfected cells were maintained for 48 h prior to experimentation.

Bioluminescence resonance energy transfer^2 (BRET^2)

Interactions between CB_1 and arrestin2 were quantified *via* $BRET^2$ according to previously described methods (Laprairie *et al*., 2014a). BRET efficiency ($BRET_{Eff}$) was determined as previously described (James *et al*., 2006; Laprairie *et al*., 2014a) such that Rluc alone was used to calculate $BRET_{MIN}$ and the Rluc-GFP^2 fusion protein was used to calculate $BRET_{MAX}$.

On- and In-cell™ western

On-cell™ western analyses were completed as described previously (Laprairie *et al*., 2014a) using primary antibody directed against N-CB_1 (1:500; Cayman Chemical Company, Ann Arbor, MI, Cat No. 101500). All experiments measuring CB_1 included an N-CB_1 blocking peptide control (1:500; Cayman Chemical Company), which was incubated with N-CB_1 antibody (1:500). Immunofluorescence observed with the N-CB_1 blocking peptide was subtracted from all experimental replicates. In-cell™ western analyses were conducted as described previously (Laprairie *et al*., 2014a). Primary antibody solutions were: N-CB_1 (1:500), pERK1/2(Tyr205/185) (1:200), ERK1/2 (1:200), pPLCβ3(S537) (1:500), PLCβ3 (1:1000), or β-actin (1:2000) (all from Santa Cruz Biotechnology, Santa Cruz, CA). Secondary antibody solutions were: $IR^{CW700dye}$ or $IR^{CW800dye}$ (1:500; Rockland Immunochemicals, Gilbertsville, PA). Quantification was completed using the Odyssey Imaging system and software (v. 3.0; Li-Cor, Lincoln, NE).

Data analysis and curve fitting

Data are presented as the mean ± the standard error of the mean (SEM) or mean and 95% confidence interval, as indicated, from at least 4 independent experiments. All data analysis and curve fitting was carried out using GraphPad Prism (v. 5.0). Concentration-response curves (CRC) were fit with the non-linear regression with variable slope (4 parameters), Gaddum/Schild EC_{50} shift model, or operational model of allosterism (Eq. 1) (Keov *et al.,* 2011) and are shown in each figure according to the best-fit model as determined by R^2 value (GraphPad Prism v. 5.0). Pharmacological statistics were obtained from non-linear regression models as indicated in figures and tables. Global curve fitting of allosterism data was carried out using the following operational model (Hudson *et al*., 2014; Keov *et* al., 2011; Smith *et al.,* 2011):

$$E=\frac{E_{max}(\tau_A[A](K_B+\alpha\beta[B])+\tau_B[B]K_A)^n}{([A]K_B+K_AK_B+[B]K_A+\alpha[A][B])^n+(\tau_A[A](K_B+\alpha\beta[B])+\tau_B[B]K_A)^n} \quad \textbf{Eq. 1}$$

where E is the measured response, A and B are the orthosteric and allosteric ligand concentrations, respectively, E_{max} is the maximum system response, α is a measure of the allosteric co-operativity on ligand binding, β is a measure of the allosteric effect on efficacy, K_A and K_B are estimates of the binding of the orthosteric and allosteric ligands, respectively, n represents the Hill slope, and τ_A and τ_B represent the abilities of the orthosteric and allosteric ligands to directly activate the receptor (Smith *et* al., 2011). To fit experimental data to this equation, E_{max} and n were constrained to 1.0 and 1.0, respectively, which allowed for estimates of α, β, K_A, K_B, τ_A and τ_B.

Relative receptor activity (RA) was calculated according to equation 2 (Christopoulos and Kenakin, 2002):

$$RA = \frac{(E_{max}\%)(EC_{50\ Agonist\ Alone})}{(E_{max\ Agonist\ Alone}\%)(EC_{50})} \quad \textbf{Eq. 2}$$

where E_{max} % is the E_{max} of the concentration-response curve in the presence of a given concentration of CBD, EC_{50} is the EC_{50} (μM) in the presence of a given concentration of CBD; $E_{max\ Agonist\ Alone}$ % is the E_{max} in the absence of CBD; $EC_{50\ Agonist\ Alone}$ is the EC_{50} (μM) in the absence of CBD. Statistical analyses were one- or two-way analysis of variance (ANOVA), as indicated, using GraphPad. *Post-hoc* analyses were performed using Dunnett's multiple comparisons, Bonferroni's or Tukey's tests, as indicated. Homogeneity of variance was confirmed using Bartlett's test. The level of significance was set to $P < 0.001$ or < 0.01, as indicated. To improve the readability of the data, all figures have been laid out such that data from HEK 293A cells appears above data from ST*Hdh*$^{Q7/Q7}$ cells, and data for O-2050 appears before data for CBD (Fig. 1-3).

Results

CB_1 internalization and kinetic experiments

We had previously observed that CBD reduced CB_1 internalization in ST*Hdh*$^{Q7/Q7}$ cells (Laprairie *et al*., 2014a). Here, were sought to determine how CBD affected the kinetics of CB_1 internalization and arrestin2 recruitment in ST*Hdh*$^{Q7/Q7}$ cells. The fraction of CB_1 at the plasma membrane was dose-dependently decreased by THC (Fig. 1A) and 2-AG in ST*Hdh*$^{Q7/Q7}$ cells (Fig. 1B). The efficacy and potency of THC- and 2-AG-dependent CB_1 internalization were reduced by increasing concentrations of CBD (Fig. 1A,B). $BRET^2$ between arrestin2-Rluc and CB_1-GFP^2 was measured every 10 s for 4 min in ST*Hdh*$^{Q7/Q7}$ cells treated with 1 μM THC (Fig. 1C) or 2-AG (Fig. 1D). Increasing concentrations of CBD decreased the rate of association between arrestin2 and CB_1 over 4 min (Fig. 1E) and decreased maximal $BRET_{Eff}$ observed at 10 min (Fig. 1C-E). The fraction of CB_1 at the plasma membrane was also reduced in ST*Hdh*$^{Q7/Q7}$ cells treated with 1 μM THC (Fig. 1F) or 2-AG (Fig. 1G) over 60 min. CBD alone increased the fraction of CB_1 at the membrane (Fig. 1F-H). The rates of CB_1 internalization, and the maximum fraction of CB_1 internalized were reduced by increasing concentrations of CBD (Fig. 1F-H). Similarly, Cawston *et al*. (2013) observed that the rate of arrestin recruitment to CB_1 was reduced by the allosteric modulator Org27569. Therefore, CBD delayed interactions between CB_1 and arrestin2 and increased the pool of receptors present at the plasma membrane at sub-micromolar concentrations, which is similar to the actions of the previously described CB_1 allosteric modulator Org27569 (Cawston *et al*., 2013).

CB_1-arrestin2 $BRET^2$ experiments

2-AG and THC enhance the interaction between CB_1 and arrestin2, as indicated by $BRET^2$ in ST*Hdh*$^{Q7/Q7}$ cells (Laprairie *et al*., 2014a). Here, we used HEK 293A cells as a

heterologous expression system for CB_1 and arrestin2 to determine whether CBD acted as a NAM of CB_1. Treatment of HEK 293A cells with 0.01 – 5.00 μM THC or 2-AG for 30 min produced a dose-dependent increase in $BRET_{Eff}$ between arrestin2-Rluc and CB_1-GFP[2] (Fig. 2A-D). The CB_1 antagonist O-2050 (0.01 – 5.00 μM) produced a dose-dependent rightward shift in the THC and 2-AG CRCs that were best fit using the Gaddum/Schild EC_{50} non-linear regression model indicative of competitive antagonism (Fig. 2A,B). CBD (0.01 – 5.00 μM) treatment produced a dose-dependent rightward and downward shift in the THC and 2-AG CRCs that were best fit using the operational model of allosterism (Eq.1, Fig. 2C,D). The rightward shift in EC_{50} was significant at 1.00 μM and 0.50 μM CBD for THC- and 2-AG-treated cells, respectively (Table 1). The decrease in E_{max} was significant at 0.10 and 0.50 μM for THC- and 2-AG-treated cells, respectively (Table 1). The Hill coefficient (n) was less than 1 at 0.10 and 0.50 μM for THC- and 2-AG-treated cells, respectively (Table 1). Relative receptor activity (estimated using Eq. 2) was significantly reduced at 0.01μM for THC- and 2-AG-treated cells (Table 1). Schild analyses of these data demonstrated that while O-2050 behaved as a competitive antagonist, inhibition of $BRET_{Eff}$ by CBD was non-linear for THC- and 2-AG-treated HEK 293A cells (Fig. 2E, Table 2). These data demonstrated that CBD behaved as a NAM of THC- and 2-AG-mediated arrestin2 recruitment to CB_1 in the HEK 293A heterologous expression system.

The NAM properties of CBD on CB_1-arrestin2 interactions were confirmed in the ST*Hdh*$^{Q7/Q7}$ cell culture model of medium spiny projection neurons. As in HEK 293A cells, O-2050 treatment produced a dose-dependent rightward shift in the THC and 2-AG CRCs that were best fit using the Gaddum/Schild EC_{50} non-linear regression model indicative of competitive antagonism (Fig. 2F,G), and CBD treatment produced a dose-dependent rightward and downward shift in the THC and 2-AG CRCs that were best fit using the operational model of allosterism (Fig. 2H,I) in ST*Hdh*$^{Q7/Q7}$ cells. The rightward shift in EC_{50} was significant at 0.50 μM CBD for THC- and 2-AG-treated cells (Table 1). The decrease in E_{max} was significant at 1.00 and 5.00 μM for THC- and 2-AG-treated cells, respectively (Table 1). The Hill coefficient (n) was less than 1 at 5.00 and 0.50 μM for THC- and 2-AG-treated cells, respectively (Table 1). Relative receptor activity (Eq. 2) was significantly reduced at 0.10 μM for both THC- and 2-AG-treated cells (Table 1). The Schild regression for these data demonstrated that O-2050 modeled competitive antagonism for THC- and 2-AG-treated ST*Hdh*$^{Q7/Q7}$ cells (greater slope and R^2) (Fig. 2J, Table 2). CBD alone displayed weak partial agonist activity in this assay at concentrations > 2 μM (Suppl Fig. 1). Taken together these data indicate that CBD behaved as a NAM of THC- and 2-AG-mediated arrestin2 recruitment to CB_1 at concentrations below its reported affinity to CB_1 in a cell culture model endogenously expressing CB_1 (Pertwee, 2008).

CB_1-mediated phosphorylation of PLCβ3

THC and 2-AG treatment both result in a dose-dependent increase in PLCβ3 phosphorylation in HEK 293A cells (Fig. 3A-D) and ST*Hdh*$^{Q7/Q7}$ cells (Laprairie *et al.*, 2014a; Fig. 3F-I). O-2050 treatment resulted in a dose-dependent rightward shift in the THC and 2-AG CRCs (Fig. 3A,B,F,G), while CBD treatment resulted in a rightward and downward shift in the THC and 2-AG CRCs, in both cell lines (Fig. 3C,D,H,I). O-2050 CRCs were best fit with the Gaddum/Schild EC_{50} model, while CBD CRCs were best fit with the operational model of allosterism. The rightward shift in EC_{50} was significant at 0.50 μM CBD for THC- and 2-AG-treated HEK 293A cells (Table 3) and 0.50 and 1.00 μM CBD for THC- and 2-AG-treated ST*Hdh*$^{Q7/Q7}$ cells, respectively (Table 3). The decrease in E_{max} was significant at 1.00 and 0.50 μM for HEK 293A and ST*Hdh*$^{Q7/Q7}$ cells, respectively (Table 3). The Hill coefficient (n) was less than 1 at 0.50 μM for THC- and 2-AG-treated in both HEK 293A and ST*Hdh*$^{Q7/Q7}$ cells (Tables 1 and 3). Relative receptor activity was significantly reduced at 0.10 μM for THC- and 2-AG-treated HEK 293A and ST*Hdh*$^{Q7/Q7}$ cells (Table 3).

The Schild regression for these data demonstrated that O-2050 modeled competitive antagonism for THC- and 2-AG-treated ST*Hdh*$^{Q7/Q7}$ cells, while CBD did not (greater slope and R^2) (Fig. 3E,J, Table 2). As with arrestin2 recruitment, CBD alone was a weak partial agonist at concentrations > 2 μM (Suppl Fig. 1). In the presence of 2-AG or THC, CBD was a NAM of PLCβ3 phosphorylation in HEK 293A cells overexpressing CB_1 and ST*Hdh*$^{Q7/Q7}$ cells endogenously expressing CB_1.

CB_1-mediated phosphorylation of ERK1/2

2-AG treatment results in the phosphorylation of ERK1/2 in ST*Hdh*$^{Q7/Q7}$ cells, while THC does not (Laprairie *et al*., 2014a). 2-AG treatment produced a dose-dependent increase in ERK1/2 phosphorylation in both HEK 293A and ST*Hdh*$^{Q7/Q7}$ cells (Fig. 4A,B,D,E). O-2050 treatment resulted in a dose-dependent rightward shift in the 2-AG CRCs (Fig. 4A,D), while CBD treatment resulted in a rightward and downward shift in the 2-AG CRCs, in both cell lines (Fig. 4B,E). O-2050 CRCs were best fit with the Gaddum/Schild EC_{50} model, while CBD CRCs were best fit with the operational model of allosterism. The rightward shift in EC_{50} was significant at 0.50 and 1.00 μM CBD for HEK 293A and ST*Hdh*$^{Q7/Q7}$ cells, respectively (Table 4). The decrease in E_{max} was significant at 5.00 and 1.00 μM for HEK 293A and ST*Hdh*$^{Q7/Q7}$ cells, respectively (Table 4). The Hill coefficient (n) was less than 1 at 0.10 and 0.01 μM CBD for HEK 293A and ST*Hdh*$^{Q7/Q7}$ cells, respectively (Table 4). Relative receptor activity was significantly reduced at 0.10 and 0.01 μM for 2-AG-treated HEK 293A and ST*Hdh*$^{Q7/Q7}$ cells, respectively (Table 4). The Schild regression for these data demonstrated that O-2050 modeled competitive antagonism in HEK293A (Fig. 3C) and ST*Hdh*$^{Q7/Q7}$ (Fig. 4F) cells, whereas CBD did not (greater slope and R^2) (Table 2). CBD was a NAM of 2-AG-mediated ERK1/2 phosphorylation in HEK 293A cells overexpressing CB_1 and ST*Hdh*$^{Q7/Q7}$ cells endogenously expressing CB_1 at lower concentrations than those reported for CB_1 agonist activity (Mechoulam *et al*., 2007; McPartland *et al*., 2014) (Suppl Fig. 1). Therefore, CBD behaved as a NAM in these cell lines for arrestin2 recruitment, PLCβ3 and ERK1/2 phosphorylation.

Operational modeling of allosterism

While O-2050 acted as a competitive orthosteric antagonist, CBD acted as a NAM in arrestin2, PLCβ3, and ERK1/2 assays. Global curve fitting of data to the operational model of allosterism was used to assess the NAM activity of CBD. Data were fit to this model by constraining E_{max} and n (Hill slope) to 1.0 and 1.0, respectively. In this way, the allosteric co-operativitiy coefficient for ligand binding (α) was found to be less than 1.0 (0.37), with no significant difference between cell lines, orthosteric ligands, or assays (Table 5) indicating that CBD acted as a NAM to reduce the binding of THC and 2-AG. CBD also reduced the efficacy of the orthosteric ligand because β (co-operativitiy coefficient for ligand efficacy) was consistently less than 1 (0.44). Based on the estimated value of orthosteric ligand affinity (K_A) and the ability of the orthosteric ligand to activate CB_1 (τ_A), 2-AG (241 nM) and THC (97 nM) were able to directly activate CB_1 within a similar concentration range to previously published data (reviewed in Pertwee, 2008). CBD did not display agonist activity, as shown by the estimate of τ_B, but exhibited a greater estimated affinity (304 nM) for CB_1 (K_B) than would be predicted for the orthosteric site (reviewed in Pertwee, 2008). β and αβ can be used to assess ligand bias (functional selectivity) for allosteric modulators (Keov *et al*., 2011). No differences in β and αβ were observed in HEK 293A cells in all assays (Table 5). In ST*Hdh*$^{Q7/Q7}$ cells, β and αβ were reduced in PLCβ3 assays compared to arrestin2 recruitment and ERK assays, indicating that CBD was a functionally selective inhibitor of arrestin2 and ERK1/2 pathways (Table 5). Overall, CBD was a NAM of orthosteric ligand binding and efficacy at CB_1.

Negative allosteric modulation of antagonist binding

If CBD reduced the binding of orthosteric agonists to CB_1, as predicted by the operational model of allosterism, then CBD should also reduce the binding of CB_1 inverse agonists and antagonists. In order to test this hypothesis, ST*Hdh*$^{Q7/Q7}$ cells were treated with the CB_1 inverse agonist AM251 (Pertwee, 2005) and CBD and ERK phosphorylation was measured (Fig. 5A). CBD treatment resulted in a rightward and upward shift in the AM251 CRC (Fig. 5A). CBD CRCs were best fit with the operational model of allosterism. To further test our hypothesis, ST*Hdh*$^{Q7/Q7}$ cells were treated with 2-AG and 500 nM O-2050, 500 nM CBD, or 500 nM O-2050 *and* 500 nM CBD (Fig 5B). Treatment of ST*Hdh*$^{Q7/Q7}$ cells with 2-AG, O-2050 and CBD produced a CRC that was shifted right and down relative to 2-AG alone and left relative to 2-AG and O-2050, indicating that CBD had reduced the competitive antagonistic activity of O-2050 and reduced the efficacy of 2-AG (Fig. 5B). Therefore, CBD was a NAM of orthosteric ligand binding as demonstrated by the reduced potency and efficacy of the CB_1 inverse agonist AM251 and the antagonist O-2050.

Mutagenesis of CB_1

The CB_1 splice variants CB_{1A} and CB_{1B} differ in the first 89 amino acids of the N-terminus relative to CB_1. We compared the allosteric activity of CBD in ST*Hdh*$^{Q7/Q7}$ cells expressing CB_1, CB_{1A} and CB_{1B} using BRET^2. $BRET_{Eff}$ did not differ between CB_1-GFP^2, CB_{1A}-GFP^2, and CB_{1B}-GFP^2-expressing cells treated with 0.01 – 5.00 μM THC or 2-AG ± 0.5 μM O-2050 or 5.00 μM CBD (Suppl Fig. 2A,B). Therefore, the allosteric activity of CB_1 is not contained within amino acids 1 – 89 that differ between CB_1, CB_{1A}, and CB_{1B}, but is associated with the conserved residues common to all three variants (Bagher *et al*., 2013; Fay and Farrens, 2013).

Fay and Farrens (2013) previously reported that Cys-98 and Cys-107 in the extracellular N-terminus of CB_1 contribute to the allosteric activity of ORG27569 and PSNCBAM-1. They suggested that these residues form a disulfide bridge, which contributed to allosteric modulator activity of ORG27569 and PSNCBAM-1 (Fay and Farrens, 2013). We hypothesized that these residues might similarly influence the allosteric activity of CBD. We wanted to determine whether it was the polarity of Cys-98 and Cys-107 or the formation of a disulfide bridge that contributed to allosteric activity. Each of these residues was individually mutagenized to Ala or Ser in the CB_1-GFP^2 plasmid (CB_1^{WT}-GFP^2, CB_1^{C98A}-GFP^2, CB_1^{C107A}-GFP^2, CB_1^{C98S}-GFP^2, CB_1^{C107S}-GFP^2) and transfected with arrestin2-Rluc into ST*Hdh*$^{Q7/Q7}$ cells. Treatment of CB_1^{WT}-, CB_1^{C98A}-, CB_1^{C107A}-, CB_1^{C98S}-, or CB_1^{C107S}-expressing cells with 0.01 – 5.00 μM THC or 2-AG alone resulted in a response that did not differ between CB_1 mutants or between THC and 2-AG treatments (Fig. 6A,B). Further, the competitive antagonistic activity of 0.50 μM O-2050 was not different in CB_1 mutant expressing-cells treated with 0.01 – 5.00 μM THC or 2-AG (Suppl Fig. 2C,D). Together, these data indicated that mutation of Cys-98 or Cys-107 did not alter CB_1 response to orthosteric ligand. Treatment of CB_1^{WT}-expressing cells with 0.01 – 5.00 μM THC or 2-AG and 5.00 μM CBD resulted in a rightward and downward shift in the $BRET_{Eff}$ CRCs (Fig. 6A,B). Similarly, treatment of CB_1^{C98A}- or CB_1^{C107A}-expressing cells with 0.01 – 5.00 μM THC or 2-AG and 5.00 μM CBD resulted in a rightward and downward shift in the $BRET_{Eff}$ CRCs compared to vehicle treatment (Table 6). The magnitude of the rightward and downward shift was less pronounced in CB_1^{C98A}- and CB_1^{C107A}- compared to CB_1^{WT}-, CB_1^{C98S}-, and CB_1^{C107S}-expressing cells treated with CBD (Table 6; Fig. 6A,B). The presence of a polar Ser or Cys at positions 98 or 107 was sufficient to recover the wild-type response to CBD. Therefore, the allosteric activity of CBD at CB_1 depended in part on the presence of polar residues at positions 98 and 107, independent of a disulfide bridge. Additional residues common to CB_1, CB_{1A}, and CB_{1B} may also contribute to the allosteric effect of CBD (Fig. 6C).

Discussion and Conclusions

Cannabidiol behaves as a negative allosteric modulator of CB_1

In this study, we provide *in vitro* evidence for the non-competitive negative allosteric modulation of CB_1 by CBD. CBD treatment resulted in negative co-operativity ($\alpha < 1$) and reduced orthosteric ligand (THC and 2-AG) efficacy ($\beta < 1$) at concentrations lower than the predicted affinity of CBD for the orthosteric binding site at CB_1 [304 nM (this study) *versus* > 4 μM (reviewed in Pertwee, 2008)]. As a NAM of CB_1 orthosteric ligand-dependent effects, CBD reduced both G protein-dependent signaling and arrestin2 recruitment, which explains both the diminished signaling and diminished BRET observed between CB_1-GFP^2 and arrestin2-Rluc. In contrast to the NAM activity of CBD, and as shown previously, O-2050 acted as a competitive orthosteric antagonist of CB_1 (Canals and Milligan, 2008; Higuchi *et al.,* 2010; Hudson *et al.*, 2010; Ferreira *et al.*, 2012; Anderson *et al*., 2013; Laprairie *et al*., 2014) rather than a partial agonist (Wiley *et al*., 2011, 2012). To directly test the hypothesis that a disulfide bridge between Cys-98 and Cys-107 regulates the activity of CB_1 allosteric modulators, these residues were mutagenized to either Ala or Ser (Fay and Farrens, 2013). Mutation of these residues to Ala (non-polar) decreased the NAM activity of CBD at CB_1, but not the activity of THC, 2-AG, or O-2050. The NAM activity of CBD depended upon the presence of polar (Ser or Cys) residues at CB_1 positions 98 and 107, rather than a disulfide bridge, because replacement of either Cys residue with Ser did not change CBD NAM activity. These findings suggest that the N-terminal, extracellular residues Cys-98 and Cys-107 either partially regulate the allosteric activity of CBD at CB_1 directly, or the communication between the allosteric and orthosteric sites of CB_1.

Allosteric modulators are probe-dependent, that is, the activity of the allosteric modulator depends on the orthosteric probe being used (reviewed in Christopoulos and Kenakin, 2002). ORG27569 and PSNCBAM-1 both display probe-dependence because they are more potent modulators of CP55,940 binding and CP55,940-mediated CB_1 activation than WIN55,212-2 binding and WIN55,21-2-mediated CB_1 activation (Baillie *et al*., 2013). 2-AG was chosen as an orthosteric probe in this study because it is the most abundant endocannabinoid in the brain, and therefore 2-AG would be the predominant endogenous orthosteric ligand if exogenous CBD was administered (Sugiura *et al*., 1999). THC and CBD are the most abundant phytocannabinoids in marijuana and are used together in varying ratios both medicinally and recreationally in marijuana (Thomas *et al*., 2007). Therefore, THC was selected as an alternative orthosteric probe. In HEK 293A cells, CBD did not display probe-dependence (Table 2). In ST*Hdh*$^{Q7/Q7}$ cells, CBD was a more potent NAM of CB_1-dependent arrestin2 recruitment when THC was the orthosteric probe compared to 2-AG (Table 2). No probe-dependence was observed for PLCβ3 and ERK1/2 signaling. BRET was used in this study to directly measure the association of CB_1 and arrestin2, which may be a more sensitive method for detecting probe-dependence than In-cell™ western assays that measured PLCβ3 or ERK1/2.

ST*Hdh*$^{Q7/Q7}$ cells express several effector proteins that CBD has been shown to modulate, including CB_1, $5HT_{1A}$, GPR55, μ-opioid receptors, PPARγ and FAAH, suggesting that CBD could have acted independently of CB_1 (Tetrell *et al*., 2000; Lee *et al*., 2007; Laprairie *et al*., 2014a). However, the NAM activity of CBD was also observed in HEK 293A cells that heterologously express CB_1, but do not express $5HT_{1A}$, GPR55, and μ-opioid receptors demonstrating that these effectors did not alter the actions of CBD (Ryberg *et al*., 2007). HEK 293A cells do express PPARγ, but modulation of this nuclear receptor would not affect arrestin and G protein assays used over the duration of these experiments. Importantly, the NAM activity of CBD at CB_1 was dependent on the cannabinoid agonists 2-AG and THC, suggesting that CBD was acting at CB_1. FAAH inhibition would have enhanced, not

diminished, cannabinoid efficacy, which was not observed here. Therefore, the NAM activity of CBD at CB_1 documented in this study adds to the mechanisms of action through which chronic CBD mediates its effects *in vivo*.

No significant signaling bias was observed for CBD in HEK 293A cells because allosteric ligand efficacy (β) and co-operativity (αβ) were not different among arrestin, PLCβ3, and ERK1/2 assays (Table 5). In ST*Hdh*$^{Q7/Q7}$ cells, we observed that CBD was biased for PLCβ3 signaling compared to ERK signaling and arrestin2 recruitment as indicated by reduced β and αβ values (Table 5). Previous studies have reported that ORG27569 is also biased against ERK and arrestin signaling (Ahn *et al*., 2012, 2013; Baillie *et al*., 2013). The observation that CBD-dependent bias was observed in ST*Hdh*$^{Q7/Q7}$ cells compared to HEK 293A cells suggests that heterologous expression systems may underrepresent ligand bias (Ahn *et al*., 2013; Baillie *et al*., 2013).

Cannabidiol compared to other negative allosteric modulators of CB_1

Based on the functional effects of CBD on PLCβ3, ERK, arrestin2 recruitment and CB_1 internalization, CBD behaved like the well-characterized allosteric modulators ORG27569 and PSNCBAM-1 *in vitro* (Horswill *et al*., 2007; Cawston *et al*., 2013). At higher doses (> 2 μM), CBD was able to enhance PLCβ3 and ERK phosphorylation, and arrestin2 recruitment, as well as limit CB_1 internalization, suggesting that CBD may behave as a weak partial agonist a high concentrations, as observed elsewhere (reviewed in Mechoulam *et al*., 2007; McPartland *et al*., 2014). In this study, the primary affect of CBD at CB_1 was negative allosteric modulation at concentrations below 1 μM. The studies by Price *et al*. (2005) and Baillie *et al.* (2013) demonstrated that ORG27569 and PSNCBAM-1 paradoxically reduce orthosteric ligand efficacy and potency while increasing orthosteric ligand binding affinity and duration. It is thought that, in general, increased ligand binding results in rapid desensitization of receptors (Price *et al.*, 2005; Ahn *et al*., 2013). In this study, we did not directly test receptor desensitization, or duration of ligand binding. We did, however, estimate ligand co-operativity and found that CBD, unlike ORG27569 and PSNCBAM-1, displayed negative co-operativity for ligand binding ($\alpha < 1$) (Price *et al.*, 2005; Ahn *et al*., 2013). ORG27569 and PSNCBAM-1 increase the CB_1 receptor pool at the cell surface, and in doing so may potentiate CB_1 signaling (Cawston *et al*., 2013). *In vivo*, ORG27569 reduces food intake similar to the CB_1 inverse agonist rimonabant (Gamage *et al*., 2014). However, the *in vivo* actions of ORG27569 are CB_1-independent, suggesting that the *in vitro* pharmacology of ORG27569 does not correlate with *in vivo* observations (Gamage *et al*., 2014). Like ORG27569, CBD may mediate a subset of its *in vivo* actions through non-CB_1 targets (Campos *et al*., 2012). For example, the anxiolytic and antidepressant actions of CBD may be $5HT_{1A}$-dependent, while the antipsychotic activity of CBD may be TRPV1-dependent (Bisogno *et al*., 2001; Russo *et al*., 2005; Ryberg *et al*., 2007; Campos *et al*., 2012). Regardless of whether CBD has alternative targets *in vivo*, the work shown here demonstrates that CBD can alter the activity of common endo- and phytocannabinoids at CB_1 and this action is likely to be therapeutically important.

Conclusions

In this *in vitro* study, the NAM activity of the well-known phytocannabinoid, CBD, was characterized for the first time. The data presented here support the hypothesis that CBD binds to a distinct, allosteric site on CB_1 that is functionally distinct from the orthosteric site for 2-AG and THC. Using an operational model of allosteric modulation to fit the data (Keov *et al*., 2011), we observed that CBD reduced the potency and efficacy of THC and 2-AG at concentrations lower than the predicted affinity of CBD for the orthosteric site of CB_1. Future *in vivo* studies should test whether the NAM activity of CBD explains the 'antagonist of agonists' effects reported elsewhere (Thomas *et al*., 2007). Indeed, the NAM activity of CBD may explain its utility as an anti-psychotic, anti-epileptic and anti-depressant. In conclusion, the identification of CBD as a CB_1 NAM provides new insights into the compound's medicinal value, and may be useful in the development of novel, CB_1-selective synthetic allosteric modulators or drug combinations.

Acknowledgements

The authors would like to thank Brian D Hudson for his critical analysis of this work. This work was supported by a partnership grant from CIHR, Nova Scotia Health Research Foundation (NSHRF), and the Huntington Society of Canada (HSC) (ROP-97185) to EDW, and a CIHR operating grant (MOP-97768) to MEMK. RBL is supported by studentships from CIHR, HSC, Killam Trusts, and NSHRF. AMB is supported by scholarships from Dalhousie University and King Abdul Aziz University, Jeddah, Saudi Arabia.

All nomenclature conforms to the *British Journal of Pharmacology*'s *Guide to Receptors and Channels* (Alexander *et al*., 2009).

Statement of conflicts of interest

The authors declare that they have no conflict of interest.

References

Ahn KH, Mahmoud MM, Kendall DA (2012). Allosteric modulator ORG27569 induces CB1 cannabinoid receptor high affinity agonist binding state, receptor internalization, and Gi protein-independent ERK1/2 kinase activation. J Biol Chem 287: 12070 – 82.

Ahn KH, Mahmoud MM, Shim JY, Kendall DA (2013). Distinct roles of β-arrestin 1 and β-arrestin 2 in ORG27569-induced biased signaling and internalization of the cannabinoid receptor 1 (CB1). J Biol Chem 288: 9790 – 800.

Alexander SPH, Mathie A, Peters JA (2011). Guide to Receptors and Channels (GRAC), 4th Edition. Br J Pharmacol 164 (Suppl 1): S1-S324.

Anderson RL, Randall MD, Chan SL (2013). The complex effects of cannabinoids on insulin secretion from rat isolated islets of Langerhans. Eur J Pharmacol 706: 56 – 62.

Bagher AM, Laprairie RB, Kelly ME, Denovan-Wright EM (2013). Co-expression of the human cannabinoid receptor coding region splice variants (hCB1) affects the function of hCB1 receptor complexes. Eur J Pharmacol 721: 341 – 54.

Baillie GL, Horswill JG, Anavi-Goffer S, Reggio PH, Bolognini D, Abood ME, et al. (2013). CB(1) receptor allosteric modulators display both agonist and signaling pathway specificity. Mol Pharmacol 83: 322 – 38.

Bisogno T, Hanus L, De Petrocellis L, Tchilibon S, Ponde DE, Brandi I, et al. (2001). Molecular targets for cannabidiol and its synthetic analogues: effect on vanilloid VR1 receptors and on the cellular uptake and enzymatic hydrolysis of anandamide. Br J Pharmacol 134: 845 – 52.

Campos AC, Moreira FA, Gomes FV, Del Bel EA, Guimarães FS (2012). Multiple mechanisms involved in the large-spectrurm therapeutic potential of cannabidiol in psychiatric disorders. Philos Trans R Soc Lond B Biol Sci 367: 3364 – 78.

Canals M, Milligan G (2008). Constitutive activity of the cannabinoid CB1 receptor regulates the function of co-expressed Mu opioid receptors. J Biol Chem 283: 11424 – 34.

Cawston EE, Redmond WJ, Breen CM, Grimsey NL, Connor M, Glass M (2013). Real-time characterization of cannabinoid receptor 1 (CB1) allosteric modulators reveals novel mechanism of action. Br J Pharmacol 170: 893 – 907.

Christopoulos A and Kenakin T (2002). G protein-coupled receptor allosterism and complexing. Pharmacol Rev 54: 323 – 74.

Fay JF and Farrens DL (2013). The membrane proximal region of the cannabinoid receptor CB1 N-terminus can allosterically modulate ligand affinity. Biochemistry 52: 8286 – 94.

Ferreira SG, Teixeira FM, Garção P, Agostinho P, Ledent C, Cortes L, et al. (2012). Presynaptic CB(1) cannabinoid receptors control frontocortical serotonin and glutamate release--species differences. Neurochem Int 61: 219 – 26.

Gamage TF, Ignatowska-Jankowska BM, Wiley JL, Abdelrahman M, Trembleau L, Greig IR, et al. (2014). In-vivo pharmacological evaluation of the CB1-receptor allosteric modulator Org-27569. Behav Pharmacol 25: 182 – 5.

Hayakawa K, Mishima K, Hazekawa M, Sano K, Irie K, Orito K, et al. (2008). Cannabidiol potentiates pharmacological effects of Delta(9)-tetrahydrocannabinol via CB(1) receptor-dependent mechanism. Brain Res 1188: 157 – 64.

Higuchi S, Irie K, Mishima S, Araki M, Ohji M, Shirakawa A, et al. (2010). The cannabinoid 1-receptor silent antagonist O-2050 attenuates preference for high-fat diet and activated astrocytes in mice. J Pharmacol Sci 112: 369 – 72.

Horswill JG, Bali U, Shaaban S, Keily JF, Jeevaratnam P, Babbs AJ, et al. (2007). PSNCBAM-1, a novel allosteric antagonist at cannabinoid CB1 receptors with hypophagic effects in rats. Br J Pharmacol 152: 805 – 14.

Hudson BD, Hébert TE, Kelly ME (2010). Physical and functional interaction between CB1 cannabinoind receptors and beta2-adrenoceptors. Br J Pharmacol 160: 627 – 42.

Hudson BD, Christiansen E, Murdoch H, Jenkins L, Hansen AH, Madsen O, et al. (2014). Complex pharmacology of novel allosteric free fatty acid 3 receptor ligands. Mol Pharmacol 86: 200 – 10.

James JR, Oliveira MI, Carmo AM, Iaboni A, Davis SJ (2006). A rigorous experimental framework for detecting protein oligomerization using bioluminescence resonance energy transfer. Nat Methods 3: 1001 – 6.

Kathmann M, Flau K, Redmer A, Tränkle C, Schlicker E (2006). Cannabidiol is an allosteric modulator at mu- and delta-opioid receptors. Naunyn Schmiedebergs Arch Pharmacol 372: 354 – 61.

Keov P, Sexton PM, Christopoulos A (2011). Allosteric modulator of G protein-coupled receptors: A pharmacological perspective. Neuropharmacol 60: 24 – 35.

Laprairie RB, Kelly MEM, Denovan-Wright EM (2013). Cannabinoids increase type 1 cannabinoid receptor expression in a cell culture model of medium spiny projection neurons: Implications for Huntington's disease. Neuropharmacol 72: 47 – 57.

Laprairie RB, Bagher AM, Kelly MEM, Dupré DJ, Denovan-Wright EM (2014a). Type 1 Cannabinoid Receptor Ligands Display Functional Selectivity in a Cell Culture Model of Striatal Medium Spiny Projection Neurons. J Biol Chem E-pub ahead of print.

Laprairie RB, Warford JR, Hutchings S, Robertson GS, Kelly MEM, Denovan-Wright EM (2014b). The cytokine and endocannabinoid systems are co-regulated by NF-κB p65/RelA in cell culture and transgenic mouse models of Huntington's disease and in striatal tissue from Huntington's disease patients. J Neuroimmunol 267: 61 – 72.

Lee JM, Ivanova EV, Seong IS, Cashorali T, Kohane I, Gusella JF, et al. (2007). Unbiased gene expression analysis implicates the huntingtin polyglutamine tract in extra-mitochondrial energy metabolism. PLoS Genet 3: e135.

McPartland JM, Duncan M, Di Marzo V, Pertwee R (2014). Are cannabidiol and Δ9 - tetrahydrocannabivarin negative modulators of the endocannabinoid system? A systematic review. Br J Pharmacol Epub ahead of print.

Mechoulam R, Peters M, Murillo-Rodriguez E, Hanus LO (2007). Cannabidiol—recent advances. Chem Biodivers 4: 1678 – 92.

Pertwee RG, Ross RA, Craib SJ, Thomas A (2002). (-)-Cannabidiol antagonizes cannabinoid receptor agonists and noradrenaline in the mouse vas deferens. Eur J Pharmacol 456: 99 – 106.

Pertwee RG (2005). Inverse agonism and neutral antagonism at cannabinoind CB_1 receptors. Life Sci 76: 1307 – 24.

Pertwee RG (2008). Ligands that target cannabinoid receptors in the brain: from THC to anandamide and beyond. Addict Biol 13: 147 – 59.

Pamplona FA, Ferreira J, Menezes de Lima O Jr, Duarte FS, Bento AF, Forner S, et al. (2012). Anti-inflammatory lipoxin A4 is an endogenous allosteric enhancer of CB1 cannabinoid receptor. Proc Natl Acad Sci U S A 109: 21134 – 9.

Piscitelli F, Ligresti A, La Regina G, Coluccia A, Morera L, Allarà M, et al. (2012). Indole-2-carboxamides as allosteric modulators of the cannabinoid CB1 receptor. J Med Chem 55: 5627 – 31.

Price MR, Baillie GL, Thomas A, Stevenson LA, Easson M, Goodwin R, et al. (2005). Allosteric modulation of the cannabinoid CB1 receptor. Mol Pharmacol 68: 1484 – 95.

Ross RA (2007). Allosterism and cannabinoind CB(1) receptors: the shape of things to come. Trends Pharmacol Sci 28: 567 – 72.

Russo EB, Burnett A, Hall B, Parker KK (2005). Agonistic properties of cannabidiol at 5-HT1a receptors. Neurochem Res 30: 1037 – 43.

Ryan D, Drysdale AJ, Pertwee RG, Platt B (2007). Interactions of cannabidiol with endocannabinoid signalling in hippocampal tissue. Eur J Neurosci 25: 2093 – 102.

Ryberg E, Larsson N, Sjögren S, Hjorth S, Hermansson NO, Leonova J, et al. (2007). The orphan receptor GPR55 is a novel cannabinoid receptor. Br J Pharmacol 152: 1092 – 101.

Smith NJ, Ward RJ, Stoddart LA, Hudson BD, Kostenis E, Ulven T, et al (2011). Extracellular loop 2 of the free fatty acid receptor 2 mediates allosterism of phenylacetamide ago-allosteric modulator. Mol Pharmacol 80: 163 – 73.

Sugiura T, Kodaka T, Nakane S, Miyashita T, Kondo S, Suhara Y, et al. (1999). Evidence that the cannabinoid CB1 receptor is a 2-arachidonoylglycerol receptor. Structure-activity relationship of 2-arachidonoylglycerol, ether-linked analogues, and related compounds. J Biol Chem 274: 2794 – 801.

Thomas A, Baillie GL, Phillips AM, Razdan RK, Ross RA, Pertwee RG (2007). Cannabidiol displays unexpectedly high potency as an antagonist of CB1 and CB2 receptor agonists in vitro. Br J Pharmacol 150: 613 – 23.

Trettel F, Rigamonti D, Hilditch-Maguire P, Wheeler VC, Sharp AH, Persichetti F, et al. (2000). Dominant phenotypes produced by the HD mutation in STHdh(Q111) striatal cells. Hum Mol Genet 9: 2799 – 809.

Wang X, Horswill JG, Whalley BJ, Stephens GJ (2011) Effects of the allosteric antagonist 1-(4-chlorophenyl)-3-[3-(6-pyrrolidin-1-ylpyridin-2-yl)phenyl]urea (PSNCBAM-1) on CB1 receptor modulation in the cerebellum. Mol Pharmacol 79: 758 – 67.

Wiley JL, Breivogel CS, Mahadevan A, Pertwee RG, Cascio MG, Bolognini D, et al. (2011). Structural and pharmacological analysis of O-2050, a putative neutral cannabinoid CB(1) receptor antagonist. Eur J Pharmacol 651: 96 – 105.

Wiley JL, Marusich JA, Zhang Y, Fulp A, Maitra R, Thomas BF, et al. (2012). Structural analogs of pyrazole and sulfonamide cannabinoids: effects on acute food intake in mice. Eur J Pharmacol 695: 62 – 70.

Wootten D, Christopoulos A, Sexton PM (2013). Emerging paradigms in GPCR allostery: implications for drug discovery. Nat Rev Drug Discov 12: 630 – 44.

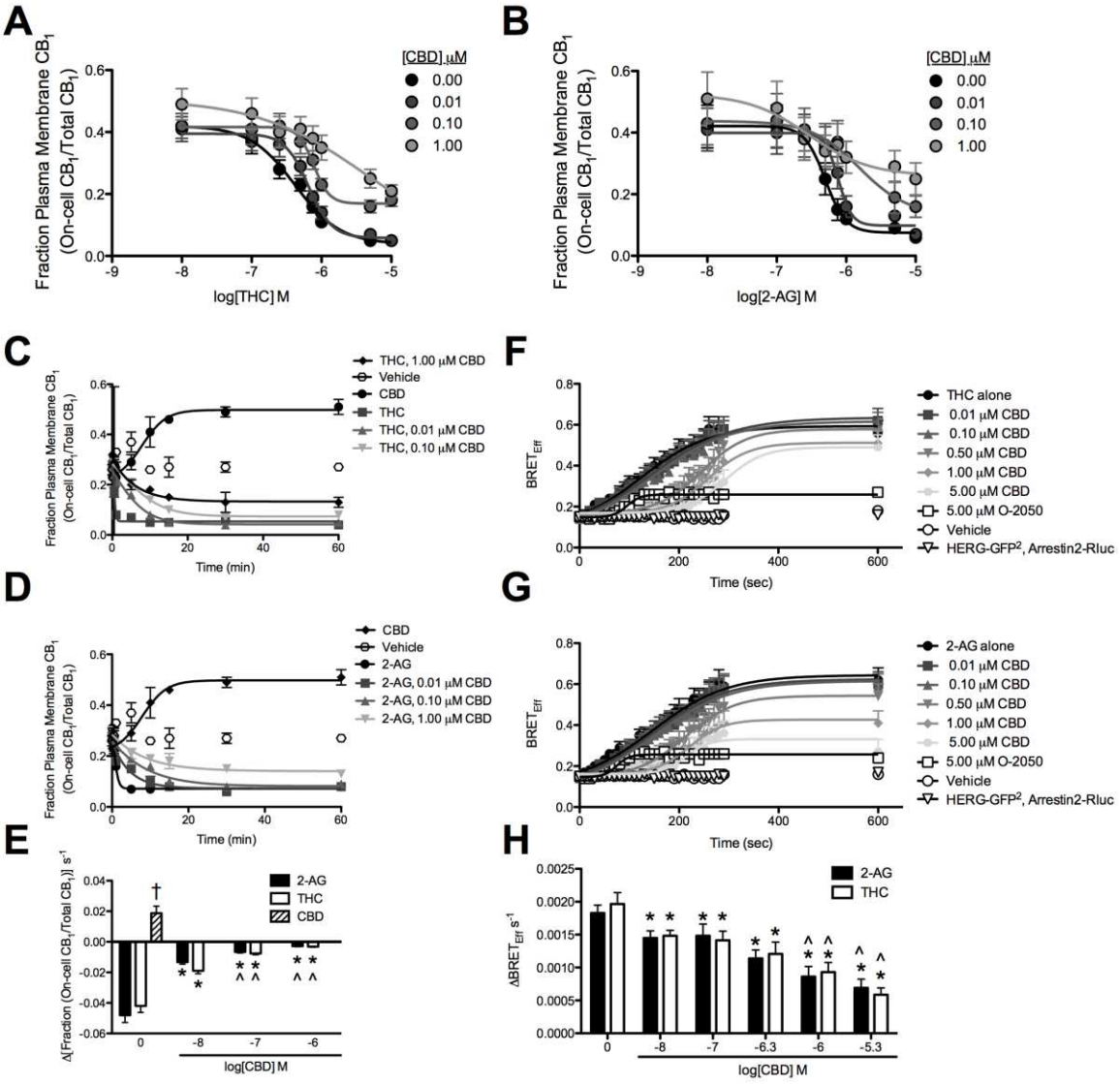

Figure 1. CBD reduced the rate and maximal $BRET_{Eff}$ between CB_1 and arrestin2 and CB_1 internalization in THC- and 2-AG-treated ST*Hdh*$^{Q7/Q7}$ cells. A,B) ST*Hdh*$^{Q7/Q7}$ cells were treated with THC **(A)** or 2-AG **(B)** ± CBD for 10 min and the fraction of CB_1 at the plasma membrane was quantified using On- and In-cell™ western analyses. Data were fit to a non-linear regression model with variable slope. **C-E)** ST*Hdh*$^{Q7/Q7}$ cells were transfected with arrestin2-Rluc- and CB_1-GFP^2-containing plasmids and $BRET^2$ was measured every 10 s for 4 min (240 sec) and again at 10 min (600 sec) after treatment with THC **(C)** or 2-AG **(D)** ± O-2050 or CBD. Data were fit to a non-linear regression model with variable slope. **E)** The rate of arrestin2 recruitment to CB_1 was measured as the change in $BRET_{Eff}$ s^{-1} during the first 4 min. **F-H)** ST*Hdh*$^{Q7/Q7}$ cells were treated with THC **(F)** or 2-AG **(G)** ± CBD for 60 min and the fraction of CB_1 at the plasma membrane was quantified using On- and In-cell™ western analyses. Data were fit to a non-linear regression model with variable slope. **H)** The rate of CB_1 internalization was measured as the change in the Fraction On-cell CB_1/Total CB_1 min^{-1} prior to plateu. †$P < 0.01$ compared to 2-AG or THC alone, *$P < 0.01$ compared to 0 CBD within orthosteric ligand treatment, ^$P < 0.01$ compared to 0.01 μM CBD (log[CBD] M = -8) within orthosteric ligand treatment, as determined *via* two-way ANOVA followed by Bonferroni's *post-hoc* test. $N = 6$.

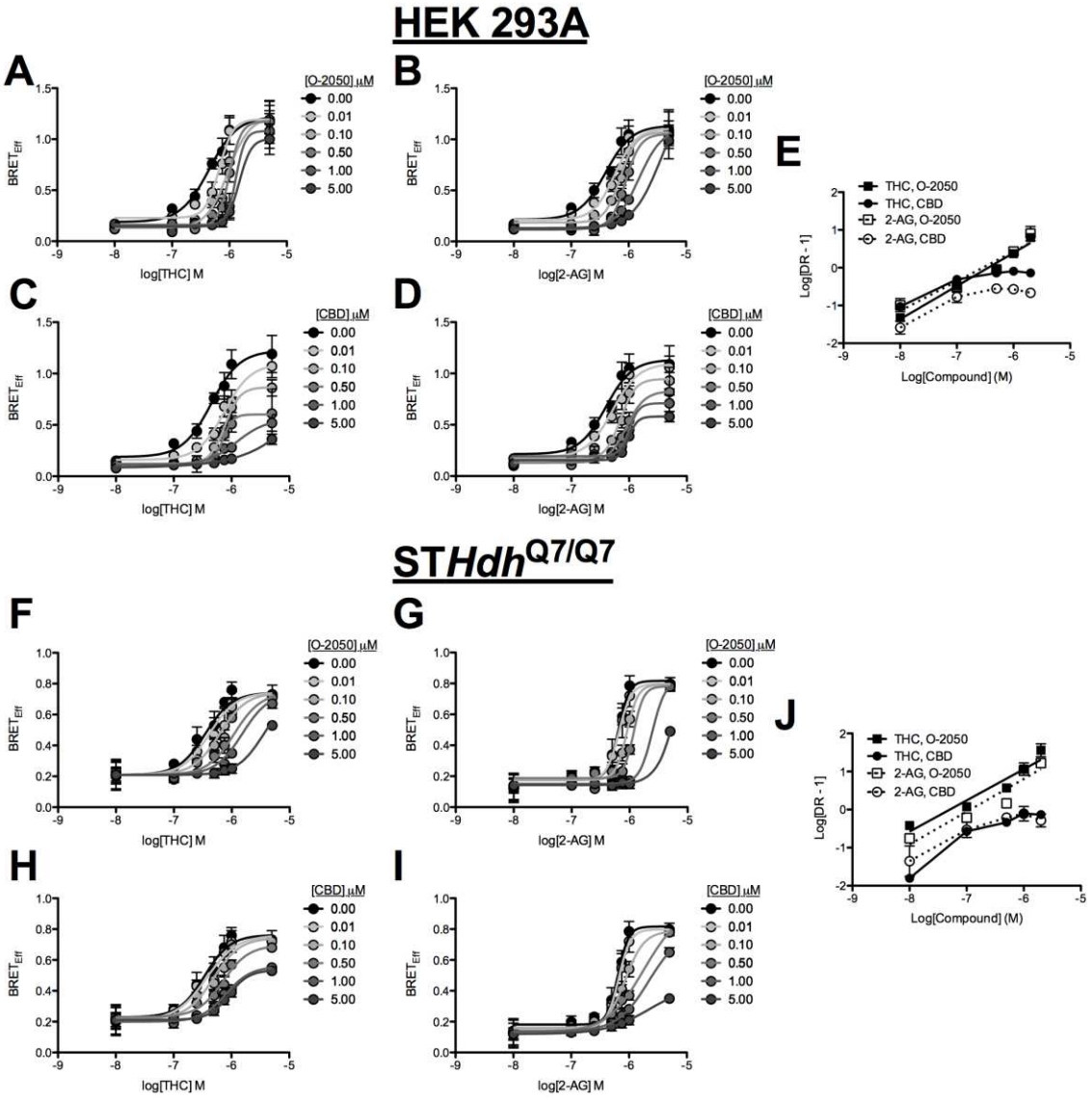

Figure 2. CBD was a NAM of arrestin2 recruitment to CB_1 following THC and 2-AG treatment. HEK 293A **(A-E)** and ST*Hdh*$^{Q7/Q7}$ **(F-J)** cells were transfected with arrestin2-Rluc- and CB_1-GFP^2-containing plasmids and BRET^2 was measured 30 min after treatment with 2-AG or THC ± O-2050 or CBD. CRCs were fit using Gaddum/Schild EC_{50} shift **(A,B,F,G)** and operational model of allosterism **(C,D,H,I)** non-linear regression models. **E,J)** Schild regressions were plotted as the logarithm of 2-AG or THC dose against the logarithm of the dose-response at $EC_{50} - 1$. $N = 6$.

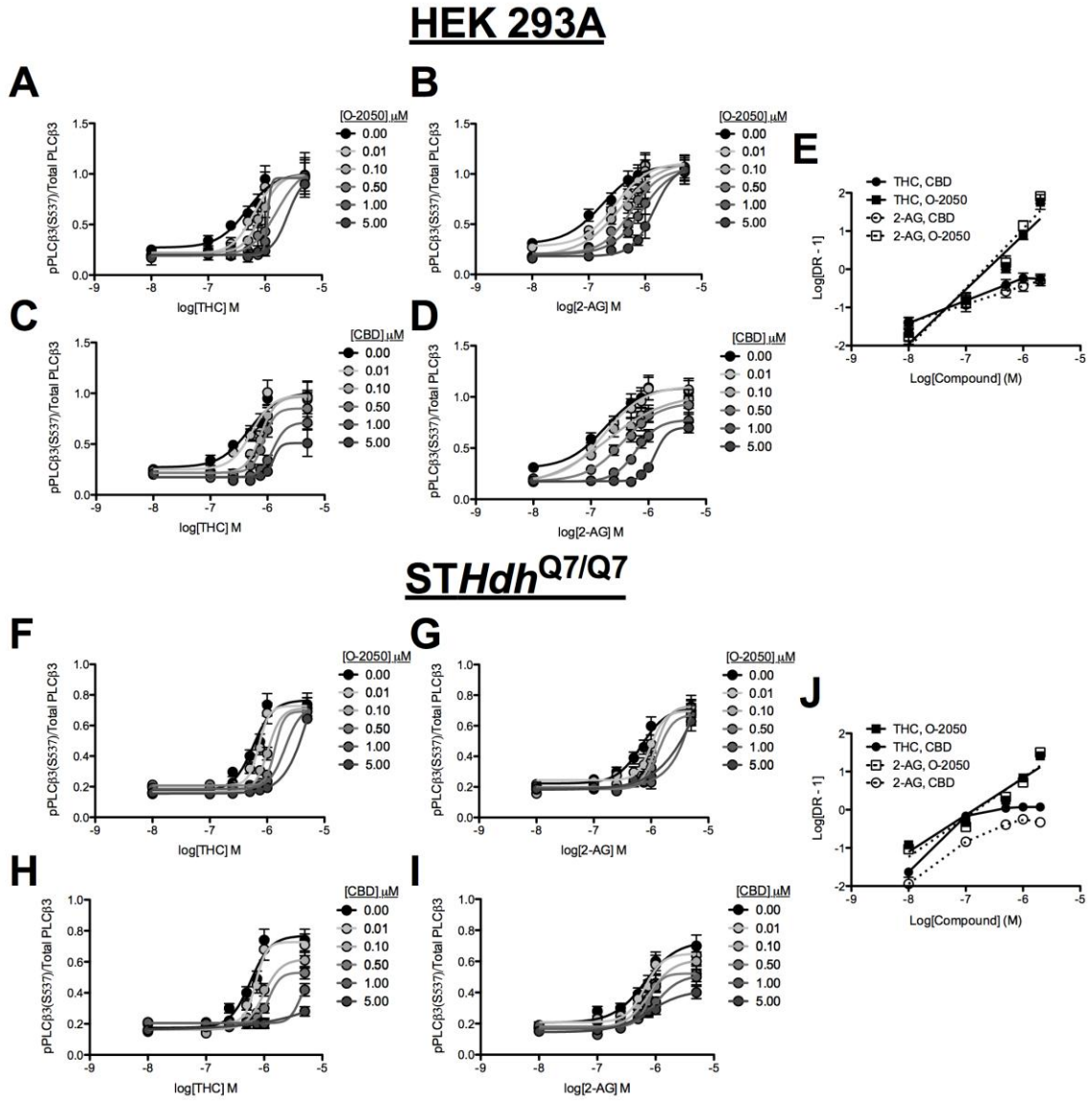

Figure 3. CBD was a NAM of CB_1-dependent PLCβ3 phosphorylation following THC and 2-AG treatment. HEK 293A cell expressing CB_1-GFP[2] **(A-E)** and ST*Hdh*$^{Q7/Q7}$ cells **(F-J)** were treated with 2-AG or THC ± O-2050 or CBD and total and phosphorylated PLCβ3 levels were determined using In-cell™ western. CRCs were fit using Gaddum/Schild EC_{50} shift **(A,B,F,G)** and operational model of allosterism **(C,D,H,I)** non-linear regression models. **E,J)** Schild regressions were plotted as the logarithm of 2-AG or THC dose against the logarithm of the dose-response at $EC_{50} - 1$. $N = 6$.

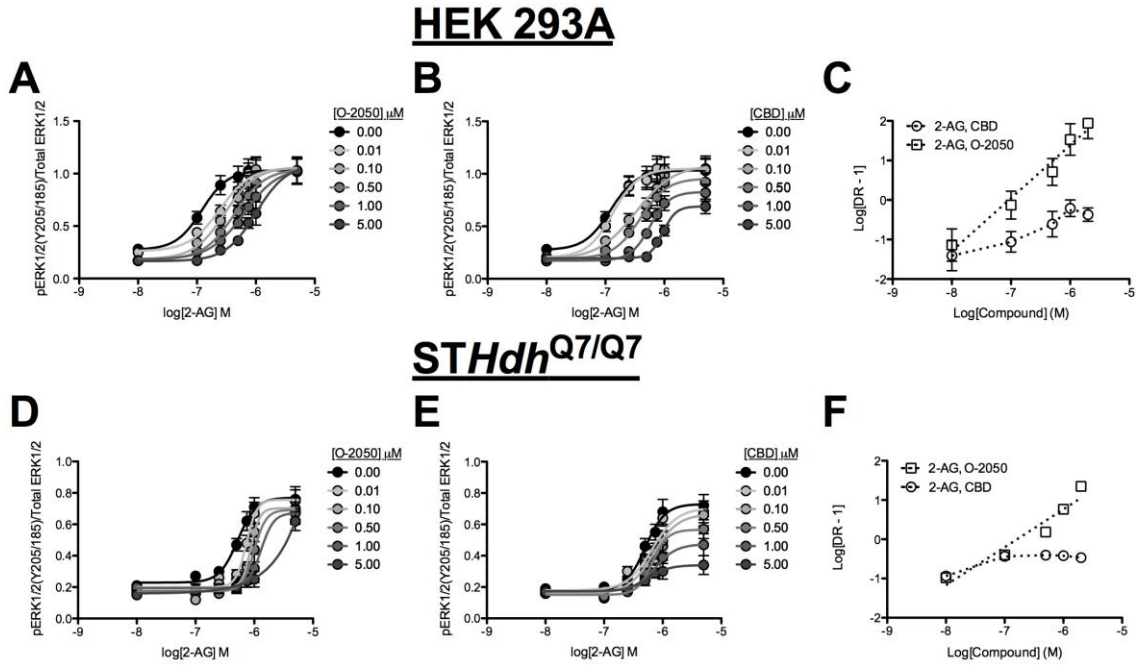

Figure 4. CBD was a NAM of CB_1-dependent ERK1/2 phosphorylation following 2-AG treatment. HEK 293A cell expressing CB_1-GFP[2] **(A-C)** and ST*Hdh*$^{Q7/Q7}$ cells **(D-F)** were treated with 2-AG ± O-2050 or CBD and total and phosphorylated ERK1/2 levels were determined using In-cell™ western. CRCs were fit using Gaddum/Schild EC_{50} shift **(A,D)** and operational model of allosterism **(B,E)** non-linear regression models. **C,F)** Schild regressions were plotted as the logarithm of 2-AG or THC dose against the logarithm of the dose-response at $EC_{50} - 1$. $N = 6$.

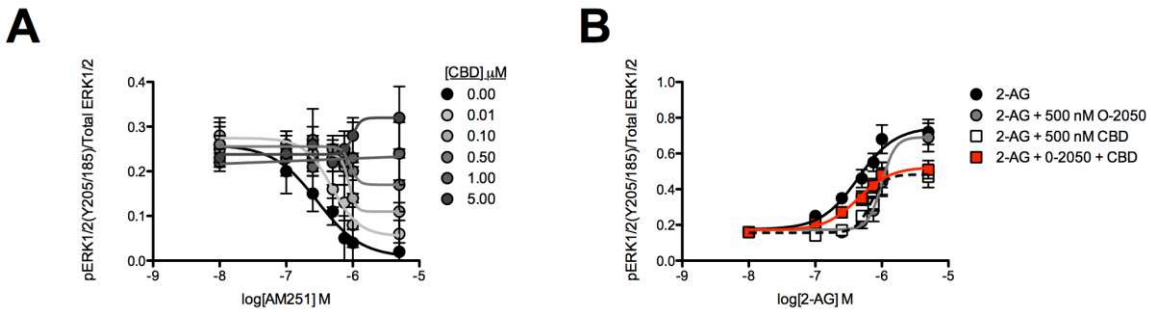

Figure 5. CBD was a NAM of AM251-depenendent inverse agonism and O-2050 antagonism. ST*Hdh*$^{Q7/Q7}$ cells were treated with AM251 ± CBD **(A)** or 2-AG ± O-2050, CBD, or O-2050 and CBD **(B)** and total and phosphorylated ERK1/2 levels were determined using In-cell™ western. CRCs were fit using the operational model of allosterism **(A)** or non-linear regression with variable slope (4 parameters) **(B)** models. $N = 6$.

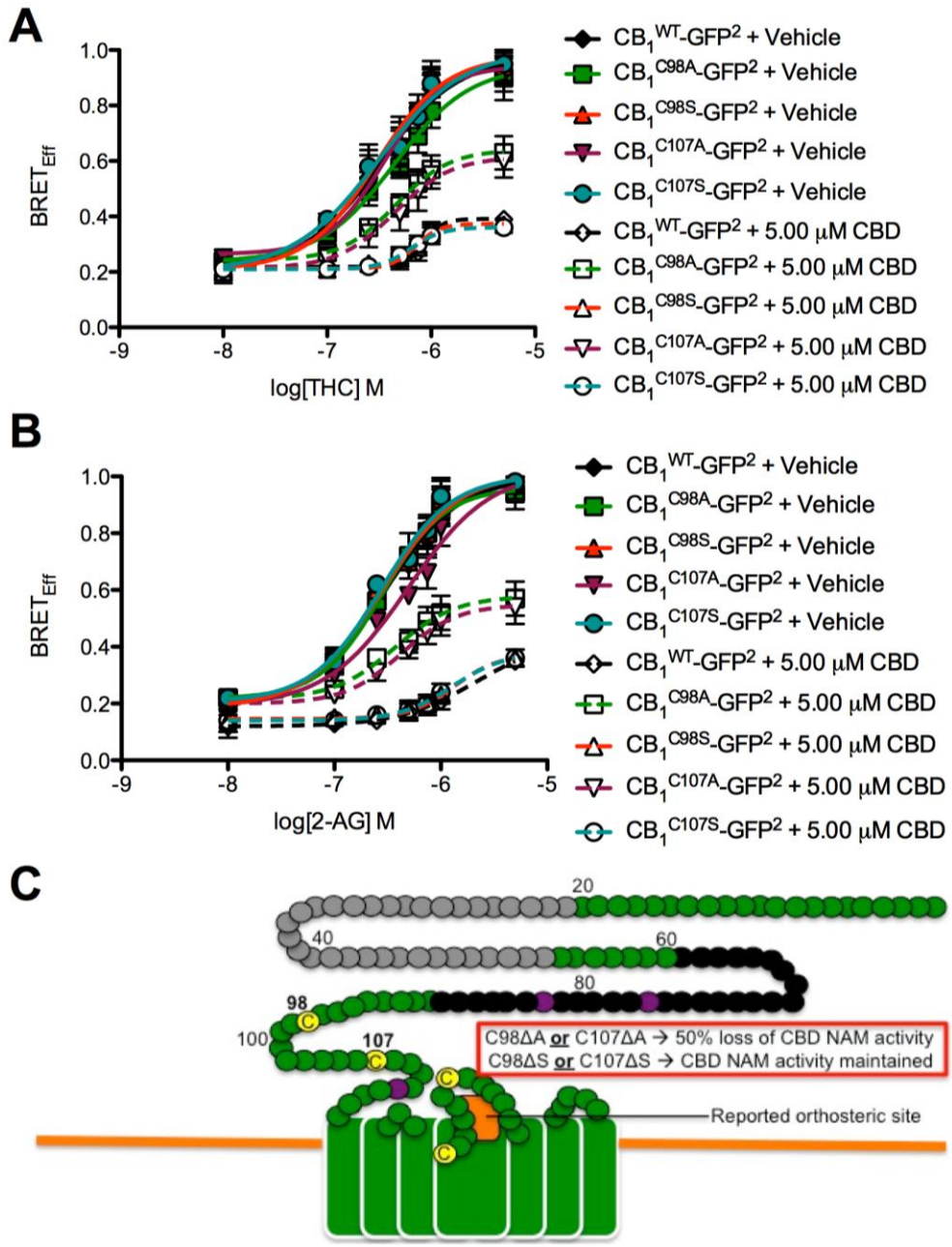

Figure 6. Cys-98 and Cys-107 coordinate the negative allosteric modulatory activity of CBD at CB_1. A,B) ST*Hdh*$^{Q7/Q7}$ cells were transfected with arrestin2-Rluc- and CB_1^{C98A}-GFP^2-, and CB_1^{C98S}-GFP^2-, CB_1^{C107A}-GFP^2-, and CB_1^{C107S}-GFP^2-containing plasmids and $BRET^2$ was measured 30 min after treatment with THC **(A)** or 2-AG **(B)** ± CBD. CRCs were fit using non-linear regression with variable slope (4 parameter) $N = 4$. **C)** Schematic of the membrane-proximal region of CB_1 summarizing data presented in this figure (adapted from Fay and Farrens, 2013). Our observations and previous studies suggest that Cys-98 and Cys-107 contribute to CB_1 allosterism, while the orthosteric site is near the second extracellular loop (orange box). In this diagram green represents extracellular surface of CB_1. Black circles represent residues unique to the N-terminus of CB_{1A}. Grey circles represent residues unique to the N-terminus of CB_{1B}. Yellow circles represent Cys. Purple circles represent N-glycosylated residues. Residues mutated in this study are marked in bold. Non-bold numbers indciate amino acid number relative to N-terminus.

TABLE 1

Effect of CBD on Arrestin-2 recruitment in HEK 293A and ST*Hdh*$^{Q7/Q7}$ cells

Data are mean ±S.E.M. or with 95% CI of four independent expreriments.

Agonist	[CBD] (μM)	EC_{50} μM (95% CI)[a]	E_{max} (95% CI)[a,b]	n (95% CI)[a,c]	RA ± S.E.M.[d]
HEK 293A					
THC	*DMSO*	0.44 (0.27 - 0.72)	1.22 (0.99 - 1.46)	1.00 (0.89 - 1.06)	1.00 ± 0.0
	0.01	0.75 (0.53 - 1.06)	1.09 (0.90 - 1.29)	0.76 (0.65 - 0.89)	0.50 ± 0.05*
	0.10	0.77 (0.64 - 0.92)	0.87 (0.75 - 0.89)†	0.63 (0.46 - 0.85)†	0.39 ± 0.04*
	0.50	0.71 (0.49 - 1.03)	0.60 (0.41 - 0.80)†	0.55 (0.43 - 0.69)†	0.29 ± 0.05*
	1.00	1.29 (0.89 - 1.41)†	0.56 (0.35 - 0.77)†	0.38 (0.26 - 0.41)†	0.15 ± 0.03*
	5.00	1.41 (1.04 - 1.77)†	0.15 (0.09 - 0.31)†	0.17 (0.08 - 0.24)†	0.04 ± 0.03*
2-AG	*DMSO*	0.39 (0.23 - 0.67)	1.13 (0.91 - 1.36)	1.00 (0.86 - 1.13)	1.00 ± 0.0
	0.01	0.52 (0.36 - 0.75)	1.10 (0.92 - 1.28)	0.81 (0.68 - 1.05)	0.72 ± 0.04*
	0.10	0.71 (0.59 - 0.86)	0.95 (0.82 - 1.07)	0.78 (0.73 - 0.93)	0.46 ± 0.07*
	0.50	0.91 (0.69 - 1.08)†	0.83 (0.59 - 1.09)†	0.64 (0.51 - 0.74)†	0.31 ± 0.02*
	1.00	1.00 (0.87 - 1.16)†	0.71 (0.63 - 0.79)†	0.33 (0.21 - 0.53)†	0.24 ± 0.04*
	5.00	1.09 (0.87 - 1.18)†	0.58 (0.52 - 0.64)†	0.27 (0.18 - 0.37)†	0.18 ± 0.02*
ST*Hdh*$^{Q7/Q7}$					
THC	*DMSO*	0.34 (0.21 - 0.46)	0.76 (0.65 - 0.88)	1.00 (0.93 - 1.31)	1.00 ± 0.0
	0.01	0.37 (0.18 - 0.56)	0.76 (0.58 - 0.93)	0.87 (0.54 - 1.24)	0.91 ± 0.3
	0.10	0.49 (0.32 - 0.66)	0.74 (0.63 - 0.86)	0.81 (0.43 - 1.07)	0.68 ± 0.1*
	0.50	0.72 (0.50 - 0.94)†	0.70 (0.59 - 0.79)	0.80 (0.35 - 1.06)	0.43 ± 0.1*
	1.00	0.80 (0.56 - 1.05)†	0.54 (0.48 - 0.64)†	0.74 (0.36 - 0.95)	0.31 ± 0.1*
	5.00	0.91 (0.70 - 1.17)†	0.50 (0.48 - 0.59)†	0.65 (0.30 - 0.84)†	0.26 ± 0.0*
2-AG	*DMSO*	0.64 (0.56 - 0.73)	0.82 (0.74 - 0.90)	1.00 (0.71 - 1.37)	1.00 ± 0.0
	0.01	0.66 (0.52 - 0.84)	0.80 (0.65 - 0.94)	0.89 (0.70 - 1.09)	0.94 ± 0.2
	0.10	0.86 (0.69 - 1.08)	0.78 (0.68 - 0.89)	0.56 (0.32 - 0.83)	0.72 ± 0.2*
	0.50	1.80 (1.42 - 2.18)†	0.76 (0.65 - 1.05)	0.29 (0.14 - 0.42)†	0.34 ± 0.1*
	1.00	2.18 (2.06 - 3.53)†	0.74 (0.68 - 1.04)	0.25 (0.16 - 0.38)†	0.27 ± 0.1*
	5.00	2.20 (1.95 - 3.55)†	0.44 (0.25 - 0.57)†	0.25 (0.18 - 0.37)†	0.16 ± 0.0*

[a]Determined using non-linear regression with variable slope (4 parameter) analysis; [b]Maximal agonist effect $BRET_{Eff}$; [c]Hill coefficient; [d]Relative Activity, as determined in Eq. 2.

†Significantly different from the DMSO vehicle as determined by non-overlapping CI.

*$P < 0.01$ compared to DMSO vehicle as determined by one-way ANOVA followed by Dunnett's multiple comparison.

TABLE 2

Schild analysis of Arrestin-2, PLCβ3, AND ERK modulation by CBD

Data are mean ±S.E.M. or with 95% CI of four independent experiments.

HEK 293A				
Agonist	Slope[a]	R^2	pA_2 (μM) ± S.E.M.[b]	IC_{50} (μM) (95% CI)[c]
BRET[2] (Arrestin-2-Rluc and CB_1-GFP[2])				
THC, O-2050	1.02 ± 0.11	0.89	0.84 ± 0.06	0.42 (0.22 - 0.64)
THC, CBD	0.54 ± 0.06*	0.62	-	0.31 (0.19 - 0.37)
2-AG, O-2050	1.06 ± 0.06	0.95	0.38 ± 0.04**	0.57 (0.29 - 0.67)
2-AG, CBD	0.54 ± 0.07*	0.41	-	0.36 (0.21 - 0.47)
$G\alpha_q$-coupled Phosphorylation of PLCβ3				
THC, O-2050	0.99 ± 0.05	0.90	1.04 ± 0.13	0.45 (0.35 - 0.58)
THC, CBD	0.59 ± 0.09*	0.68	-	0.39 (0.29 - 0.51)
2-AG, O-2050	1.03 ± 0.07	0.96	0.29 ± 0.03**	0.58 (0.31 - 0.73)
2-AG, CBD	0.48 ± 0.07*	0.38	-	0.31 (0.17 - 0.46)
$G\alpha_{I/O}$-coupled Phosphorylation of ERK1/2				
2-AG, O-2050	0.93 ± 0.15	0.88	0.26 ± 0.03	0.39 (0.09 - 0.46)
2-AG, CBD	0.15 ± 0.02*	0.62	-	0.26 (0.19 - 0.59)
ST*Hdh*$^{Q7/Q7}$				
BRET[2] (Arrestin-2-Rluc and CB_1-GFP[2])				
THC, O-2050	0.92 ± 0.09	0.95	0.83 ± 0.21	0.35 (0.27 - 0.46)
THC, CBD	0.34 ± 0.10*	0.78	-	0.23 (0.16 - 0.27)
2-AG, O-2050	0.97 ± 0.10	0.99	0.35 ± 0.13**	0.52 (0.45 - 0.59)
2-AG, CBD	0.35 ± 0.13*	0.70	-	0.63 (0.57 - 0.89)††
Phosphorylation of PLCβ3				
THC, O-2050	1.05 ± 0.17	0.97	0.93 ± 0.15	0.79 (0.42 - 0.85)
THC, CBD	0.22 ± 0.08*	0.70	-	0.94 (0.62 - 1.19)
2-AG, O-2050	1.02 ± 0.05	0.99	0.36 ± 0.09**	0.83 (0.46 - 1.17)
2-AG, CBD	0.29 ± 0.05*	0.71	-	0.96 (0.75 - 1.25)
Phosphorylation of ERK1/2				
2-AG, O-2050	1.06 ± 0.11	0.97	0.36 ± 0.06	0.87 (0.57 - 0.99)
2-AG, CBD	0.17 ± 0.08*	0.60	-	0.27 (0.18 - 0.36)†

[a,b,c]Determined using non-linear regression analysis with a Gaddum/Schild EC_{50} shift for data presented in Figs 1-3. IC_{50} determined at 1 μM agonist. pA_2 was not determined where Schild slope was different from 1.

†Significantly different from the same agonist treatment; ††significantly different from the same modulator treatment; as determined by non-overlapping CI.

*P < 0.01 compared to the same agonist treatment; **P < 0.01 compared to the same modulator treatment; as determined by one-way ANOVA followed by Dunnett's multiple comparison.

TABLE 3

Effect of CBD on PLCβ3 activation in HEK 293A and ST*Hdh*$^{Q7/Q7}$ cells

Data are mean ±S.E.M. or with 95% CI of four independent expreriments.

Agonist	[CBD] (μM)	EC_{50} μM (95% CI)[a]	E_{max} (95% CI)[a,b]	*n* (95% CI)[a,c]	RA ± S.E.M.[d]
HEK 293A					
THC	*DMSO*	0.47 (0.27 - 0.69)	1.01 (0.82 - 1.20)	1.00 (0.76 - 1.26)	1.00 ± 0.0
	0.01	0.58 (0.34 - 0.81)	0.98 (0.80 - 1.17)	0.83 (0.70 - 1.13)	0.79 ± 0.17
	0.10	0.76 (0.59 - 0.97)	0.97 (0.81 - 1.13)	0.73 (0.67 - 0.93)	0.60 ± 0.08*
	0.50	0.86 (0.70 - 1.07)†	0.85 (0.70 - 1.00)	0.54 (0.41 - 0.72)†	0.46 ± 0.05*
	1.00	1.23 (0.85 - 1.80)†	0.71 (0.63 - 0.79)†	0.36 (0.18 - 0.51)†	0.27 ± 0.03*
	5.00	1.26 (0.82 - 1.58)†	0.51 (0.41 - 0.61)†	0.16 (0.04 - 0.26)†	0.19 ± 0.02*
2-AG	*DMSO*	0.48 (0.28 - 0.72)	1.09 (0.90 - 1.29)	1.00 (0.86 - 1.15)	1.00 ± 0.0
	0.01	0.63 (0.37 - 0.96)	1.11 (0.91 - 1.30)	0.92 (0.81 - 1.02)	0.84 ± 0.07
	0.10	0.83 (0.58 - 1.03)	1.03 (0.74 - 1.32)	0.84 (0.74 - 1.00)	0.60 ± 0.07*
	0.50	1.11 (0.95 - 1.35)†	0.95 (0.80 - 1.10)	0.57 (0.46 - 0.79)†	0.41 ± 0.08*
	1.00	1.62 (1.23 - 1.51)†	0.78 (0.67 - 0.88)†	0.22 (0.07 - 0.36)†	0.23 ± 0.01*
	5.00	2.48 (1.72 - 3.22)†	0.60 (0.54 - 0.66)†	0.13 (0.04 - 0.24)†	0.12 ± 0.06*
ST*Hdh*$^{Q7/Q7}$					
THC	*DMSO*	0.58 (0.42 - 0.79)	0.77 (0.65 - 0.89)	1.00 (0.71 - 1.25)	1.00 ± 0.0
	0.01	0.72 (0.61 - 0.85)	0.73 (0.63 - 0.82)	0.54 (0.44 - 0.82)	0.77 ± 0.3
	0.10	0.99 (0.78 - 1.22)	0.62 (0.54 - 0.69)	0.51 (0.42 - 0.78)	0.48 ± 0.1*
	0.50	1.22 (0.85 - 1.57)†	0.53 (0.48 - 0.58)†	0.55 (0.23 - 0.64)†	0.33 ± 0.1*
	1.00	4.00 (2.76 - 4.32)†	0.49 (0.37 - 0.52)†	0.51 (0.17 - 0.62)†	0.10 ± 0.0*
	5.00	>5.00 †	-	< 0.50 †	0.03 ± 0.0*
2-AG	*DMSO*	0.66 (0.40 - 0.85)	0.73 (0.59 - 0.87)	1.00 (0.70 - 1.18)	1.00 ± 0.0
	0.01	0.67 (0.48 - 0.86)	0.65 (0.56 - 0.74)	0.77 (0.55 - 0.89)	0.88 ± 0.2
	0.10	0.78 (0.58 - 1.01)	0.61 (0.52 - 0.70)	0.57 (0.34 - 0.74)	0.71 ± 0.2*
	0.50	0.87 (0.63 - 0.92)	0.52 (0.46 - 0.58)†	0.39 (0.15 - 0.58)†	0.60 ± 0.1*
	1.00	1.04 (0.87 - 1.61)†	0.51 (0.43 - 0.56)†	0.39 (0.12 - 0.50)†	0.45 ± 0.1*
	5.00	1.78 (1.07 - 2.05)†	0.42 (0.32 - 0.51)†	0.36 (0.09 - 0.49)†	0.21 ± 0.0*

[a]Determined using non-linear regression with variable slope (4 parameter) analysis; [b]Maximal agonist effect $BRET_{Eff}$; [c]Hill coefficient; [d]Relative Activity, as determined in Eq. 2.

†Significantly different from the DMSO vehicle as determined by non-overlapping CI.

*$P < 0.01$ compared to DMSO vehicle as determined by one-way ANOVA followed by Dunnett's multiple comparison.

TABLE 4

Effect of CBD on ERK activation in HEK 293A and ST*Hdh*$^{Q7/Q7}$ cells

Data are mean ±S.E.M. or with 95% CI of four independent expreriments.

Agonist	[CBD] (μM)	EC_{50} μM (95% CI)[a]	E_{max} (95% CI)[a,b]	n (95% CI)[a,c]	RA ± S.E.M.[d]
HEK 293A					
2-AG	*DMSO*	0.12 (0.07 - 0.22)	1.03 (0.89 - 1.17)	1.00 (0.97 - 1.07)	1.00 ± 0.0
	0.01	0.13 (0.08 - 0.22)	1.05 (0.92 - 1.18)	0.91 (0.82 - 1.03)	0.96 ± 0.09
	0.10	0.33 (0.19 - 0.47)	1.09 (0.90 - 1.28)	0.63 (0.57 - 0.72)†	0.40 ± 0.06*
	0.50	0.39 (0.26 - 0.58)†	0.96 (0.82 - 1.10)	0.39 (0.29 - 0.58)†	0.30 ± 0.05*
	1.00	0.57 (0.45 - 0.72)†	0.83 (0.73 - 0.93)	0.27 (0.17 - 0.39)†	0.17 ± 0.05*
	5.00	0.95 (0.81 - 1.11)†	0.69 (0.61 - 0.76)†	0.19 (0.11 - 0.30)†	0.09 ± 0.02*
ST*Hdh*$^{Q7/Q7}$					
2-AG	*DMSO*	0.50 (0.37 - 0.68)	0.73 (0.63 - 0.83)	1.00 (0.91 - 1.22)	1.00 ± 0.0
	0.01	0.66 (0.44 - 0.99)	0.70 (0.58 - 0.83)	0.78 (0.57 - 0.83)†	0.74 ± 0.2*
	0.10	0.69 (0.48 - 0.95)	0.67 (0.56 - 0.77)	0.79 (0.56 - 0.77)†	0.67 ± 0.1*
	0.50	0.77 (0.52 - 0.87)	0.57 (0.48 - 0.65)	0.73 (0.63 - 0.87)†	0.56 ± 0.1*
	1.00	0.84 (0.69 - 1.21)†	0.47 (0.37 - 0.57)†	0.70 (0.46 - 0.81)†	0.44 ± 0.1*
	5.00	1.27 (0.81 - 1.47)†	0.33 (0.26 - 0.41)†	0.57 (0.27 - 0.72)†	0.30 ± 0.1*

[a]Determined using non-linear regression with variable slope (4 parameter) analysis; [b]Maximal agonist effect $BRET_{Eff}$; [c]Hill coefficient; [d]Relative Activity, as determined in Eq. 2.

†Significantly different from the DMSO vehicle as determined by non-overlapping CI.

*$P < 0.01$ compared to DMSO vehicle as determined by one-way ANOVA followed by Dunnett's multiple comparison.

TABLE 5

Operational model analysis of CBD at CB_1 in the presence of THC or 2-AG

Data are mean ±S.E.M. or with 95% CI of four independent expreriments.

HEK 293A

	$BRET_{Eff}$		pPLCβ3		pERK1/2
Agonist	THC	2-AG	THC	2-AG	2-AG
Modulator	CBD	CBD	CBD	CBD	CBD
-logα	0.47 ± 0.06	0.53 ± 0.07	0.47 ± 0.12	0.57 ± 0.11	0.48 ± 0.13
-logβ	0.25 ± 0.09	0.41 ± 0.03	0.28 ± 0.07	0.42 ± 0.09	0.30 ± 0.07
$\log\tau_A$ [a]	1.14 ± 0.26	1.04 ± 0.19	1.01 ± 0.20	1.12 ± 0.18	1.02 ± 0.12
$\log\tau_B$ [b]	0.21 ± 0.04	0.13 ± 0.05	0.25 ± 0.10	0.15 ± 0.06	0.06 ± 0.04
K_A [a] (nM)	128 (56.7 - 159)	262 (197 - 308)	91.9 (82.2 - 103)	255 (176 - 328)	236 (195 - 275)
K_B [b] (nM)	270 (148 - 349)	352 (272 - 409)	268 (197 - 292)	326 (279 - 382)	318 (255 - 369)
αβ	0.19	0.11	0.18	0.10	0.17

ST*Hdh*$^{Q7/Q7}$

	$BRET_{Eff}$		pPLCβ3		pERK1/2
Agonist	THC	2-AG	THC	2-AG	2-AG
Modulator	CBD	CBD	CBD	CBD	CBD
-logα	0.31 ± 0.09	0.23 ± 0.12	0.46 ± 0.18	0.38 ± 0.15	0.42 ± 0.13
-logβ	0.25 ± 0.08	0.33 ± 0.09	0.60 ± 0.12*	0.58 ± 0.09*	0.27 ± 0.06
$\log\tau_A$ [a]	0.78 ± 0.21	0.81 ± 0.17	0.81 ± 0.17	0.79 ± 0.12	0.74 ± 0.18
$\log\tau_B$ [b]	0.31 ± 0.11	0.21 ± 0.09	0.29 ± 0.12	0.18 ± 0.07	0.19 ± 0.05
K_A [a] (nM)	95.7 (58.6 - 118)	237 (181 - 294)	72.3 (59.1 - 107)	255 (178 - 318)	198 (137 - 238)
K_B [b] (nM)	278 (148.4 - 335)	333 (291 - 376)	259 (194 - 280)	315 (281 - 362)	329 (241 - 346)
αβ	0.28	0.28	0.09	0.11	0.20

All values estimated using the operational model of allosterism described in Eq. 1. [a]$\log\tau_A$ and K_A determined for THC or 2-AG; [b]$\log\tau_B$ and K_B determined for CBD.

*$P < 0.01$ compared to $BRET_{Eff}$ with the same agonist as determined by one-way ANOVA followed by Dunnett's multiple comparison.

TABLE 6

Effect of CBD on Arrestin-2 recruitment to mutant CB_1 in ST*Hdh*$^{Q7/Q7}$ cells

Data are mean with 95% CI of four independent expreriments.

Agonist	Receptor	Modulator	EC_{50} µM (95% CI)[a]	E_{max} (95% CI)[a,b]
THC	CB_1^{WT}	*DMSO*	0.34 (0.21 - 0.46)	0.96 (0.75 - 1.01)
		5.00 µM CBD	0.91 (0.70 - 1.17)†	0.30 (0.24 - 0.49)†
	CB_1^{C98A}	*DMSO*	0.35 (0.26 - 0.57)	0.94 (0.78 - 1.11)
		5.00 µM CBD	0.55 (0.37 - 0.67)^	0.64 (0.54 - 0.74)†^
	CB_1^{C107A}	*DMSO*	0.36 (0.23 - 0.46)	0.94 (0.82 - 1.07)
		5.00 µM CBD	0.56 (0.48 - 0.67)†^	0.61 (0.54 - 0.73)†^
	CB_1^{C98S}	*DMSO*	0.30 (0.17 - 0.41)	0.98 (0.83 - 1.12)
		5.00 µM CBD	0.97 (0.79 - 1.10)†	0.37 (0.32 - 0.42)†
	CB_1^{C107S}	*DMSO*	0.31 (0.16 - 0.48)	1.00 (0.82 - 1.18)
		5.00 µM CBD	0.91 (0.80 - 1.02)†	0.36 (0.31 - 0.41)†
2-AG	CB_1^{WT}	*DMSO*	0.64 (0.56 - 0.73)	0.82 (0.74 - 0.90)
		5.00 µM CBD	2.20 (1.95 - 3.55)†	0.44 (0.25 - 0.57)†
	CB_1^{C98A}	*DMSO*	0.62 (0.54 - 0.78)	0.96 (0.84 - 1.09)
		5.00 µM CBD	1.37 (1.09 - 1.59)†^	0.67 (0.59 - 0.71)†^
	CB_1^{C107A}	*DMSO*	0.59 (0.43 - 0.69)	1.03 (0.89 - 1.18)
		5.00 µM CBD	1.42 (1.23 - 1.64)†^	0.66 (0.58 - 0.72)†^
	CB_1^{C98S}	*DMSO*	0.68 (0.59 - 0.74)	1.01 (0.90 - 1.12)
		5.00 µM CBD	2.32 (1.97 - 2.57)†	0.37 (0.24 - 0.50)†
	CB_1^{C107S}	*DMSO*	0.67 (0.59 - 0.79)	1.00 (0.90 - 1.11)
		5.00 µM CBD	2.28 (2.14 - 2.40)†	0.38 (0.24 - 0.52)†

†Significantly different from DMSO vehicle within receptor group as determined by non-overlapping CI.
^Significantly different from response to 5.00 µM CBD and DMSO vehicle in CB_1^{WT} vehicle as determined by non-overlapping CI.